Experience With Advanced Instrumentation in a Hot Section Cascade

Frederick C. Yeh and Herbert J. Gladden
Lewis Research Center
Cleveland, Ohio

NASA

EXPERIENCE WITH ADVANCED INSTRUMENTATION IN A HOT SECTION CASCADE

Frederick C. Yeh and Herbert J. Gladden
National Aeronautics and Space Administration
Lewis Research Center
Cleveland, Ohio 44135

ABSTRACT

The Lewis Research Center gas turbine Hot Section Test Facility was developed to provide a "real engine" environment with known boundary conditions for the aerothermal performance evaluation and verification of computer design codes. This verification process requires experimental measurements in a hostile environment. The research instrumentation used in this facility are presented, and their characteristics and how they perform in this environment are discussed. The research instrumentation consisted of conventional pressure and temperature sensors, as well as thin-film thermocouples and heat flux gages. The hot gas temperature was measured by an aspirated temperature probe and by a dual-element, fast-response temperature probe. The data acquisition mode was both steady-state and time dependent. These experiments were conducted over a wide range of gas Reynolds numbers, exit gas Mach numbers, and heat flux levels. This facility was capable of testing at temperatures up to 1600 K, and at pressures up to 18 atm. These corresponded to an airfoil exit Reynolds number range of 0.5×10^6 to 2.5×10^6 based on the airfoil chord of 5.55 cm. Results are presented that characterize the performance capability and the durability of the instrumentation. Discussion will also be made on the challenge of making measurements in hostile environments. The instruments exhibited more than adequate durability to achieve the measurement profile. About 70 percent of the thin-film thermocouples and the dual-element temperature probe survived several hundred thermal cycles and up to 35 hr at gas temperatures up to 1600 K. Within the experimental uncertainty, the steady-state and transient heat flux measurements were comparable and consistent over the range of Reynolds numbers tested.

NOMENCLATURE

C	true chord length
C_p	specific ratio
f	frequency
g_c	gravitational constant
h	heat transfer coefficient
k	thermal conductivity
L	total distance along vane surface from leading-edge stagnation point, on pressure or suction surface
P	pressure
P1 to P6	measurement locations 1 to 6 on pressure surface
Q/A	heat flux
R	gas constant
Re	Reynolds number
r	vane radius from cascade center
S1 to S6	measurement locations 1 to 6 on suction surface
SP	stagnation point
T	temperature
$T_g(f)$	amplitude of gas temperature Fourier component, K
$T_w(f)$	amplitude of wall temperature Fourier component, K
V	velocity
X	surface distance measured from leading-edge stagnation point to the local measurement point
Y	specific heat ratio
μ	viscosity
ρ	density

Subscripts:

cal	calculated
e	stator exit (station 5)
g	gas
i	inside

o   outside

w   wall

4,5,6   axial stations 4, 5, or 6 (combustor exit, stator exit, and rotor exit)

Superscripts:

-      average

'   total

INTRODUCTION

Improved performance of turbojet and turbofan engines is typically accompanied by increased cycle pressure ratio and combustor exit gas temperature. Gas pressure levels of 25 to 30 atm and gas temperatures of 1600 K exist in some current operational engines, and pressure levels of 60 atm with temperatures of 2200 K are anticipated in advanced commercial engines. The continuing increases in turbine entry gas pressure and temperature of the modern gas turbine engine and its high development cost put a premium on an accurate initial aerothermal design of the turbine hot section hardware.

The design goals for commercial jet engines include high cycle efficiency, increased durability of the hot section components (i.e., lower maintenance costs), and lower operating costs. These goals are contradictory: High cycle efficiency requires minimizing the cooling air requirements, and increased durability requires minimizing metal temperatures and temperature gradients. An optimum design can be realized only through improved understanding of the flow field and the heat transfer process in the turbine gas path.

Sophisticated computer design codes are being developed which have the potential of providing the designer with significantly better initial estimates of the flow field and heat load on the hot section components. These codes are being evaluated and verified through low temperature and pressure research in cascades and wind tunnels. However, by design, these facilities do not model all of the processes that exist in a real engine environment, and therefore, the ability of the design codes to predict the interaction of the various parameters cannot be fully evaluated.

The gas turbine Hot Section Facility (HSF) at NASA Lewis Research Center provided a "real engine" environment with known boundary conditions and convenient access for advanced instrumentation to study the aerothermal performance of turbine hot section components. The thermal performance, and ultimately the life of these components in a realistic application, is dependent on the designer's ability to predict the local heat load distribution. The stator airfoil heat transfer coefficient presents a challenging situation for the designer because of the complex flow field through the turbine. Even though heat transfer on airfoils has been studied previously, there has been only limited engine data available to verify or calibrate the analytical models. The importance of accurate heat transfer data in both a test rig and an engine environment is self apparent. These data provide a means of verifying or improving the designer's prediction capability and reducing overall development costs. These, in turn, would promote longer component life and would minimize the amount of cooling air required.

This paper discusses the instrumentation used in the Hot Section Facility to obtain heat transfer and aerodynamic data. These include thin-film thermocouples, heat flux gages, a dual-element gas temperature probe, and an aspirated gas temperature probe that were used in the to obtain experimental data at the engine conditions. The tests were conducted in the HSF cascade rig at gas temperatures up to 1600 K and pressures up to 18 atm. This corresponded to a vane exit Reynolds number range of 0.5×10^6 to 2.5×10^6 based on the true chord of 5.55 cm. An uncertainty analysis was made in accordance with the method outlined by Kline and McClintock (1953). Typical results from these instruments and their estimated uncertainty are presented.

FACILITY

General Description

A physical layout of the Hot Section Facility (HSF) is shown in perspective view in Fig. 1(a). The HSF at NASA Lewis Research Center was a unique facility having fully automated control of the research rig through an integrated system of minicomputers and programmable controllers. The major components of this facility and how they interfaced together to provide a real engine environment are shown in the flow diagram in Fig. 1(b). This facility is discussed in more detail by Cochran et al. (1976), and by Gladden et al. (1985).

The main air supply system provided air at 10 atm to a nonvitiated preheater. The preheater modulated the air temperature between ambient and 560 K. A set of routing valves was used to select either of two modes of operation: (1) Using the compressor bypass system, air was provided to the test rig at 10 atm and at temperatures up to 560 K, and (2) using the compressor mode, the heat of compression provided air to the rig at up to 20 atm and at temperatures up to 730 K.
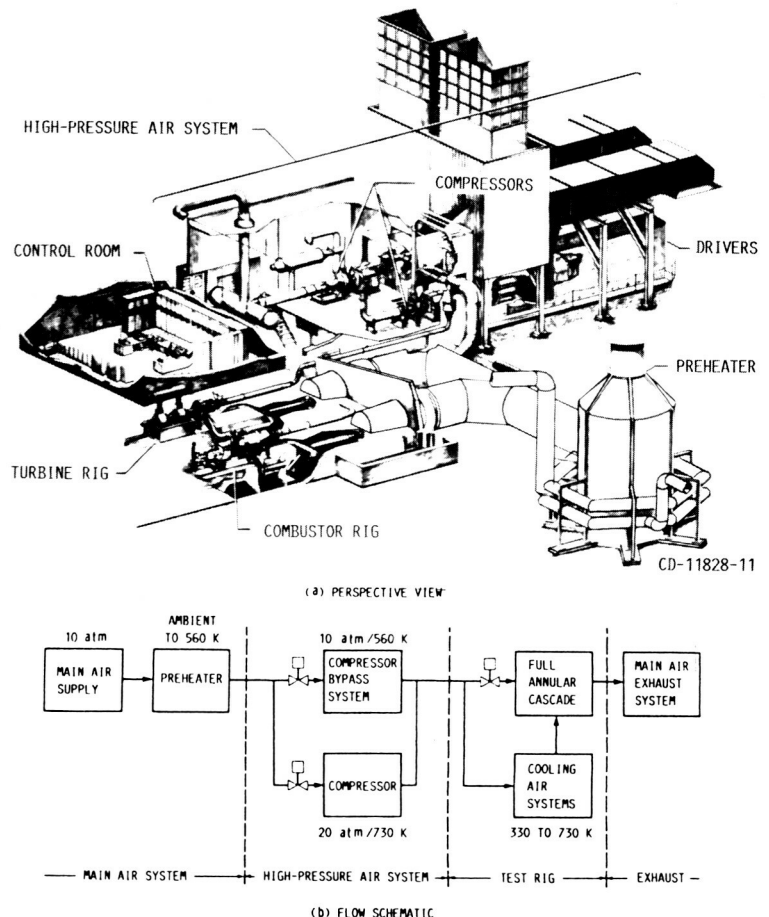

HIGH-PRESSURE AIR SYSTEM

COMPRESSORS

CONTROL ROOM

DRIVERS

PREHEATER

TURBINE RIG

COMBUSTOR RIG

CD-11828-11

(a) PERSPECTIVE VIEW

(b) FLOW SCHEMATIC

Fig. 1   Hot Section Facility

PRECEDING PAGE BLANK NOT FILMED

Cascade Configuration

The facility was configured as a stator cascade for these heat transfer and aerodynamic experiments. A cross section of the Hot Section Cascade Rig is shown in Fig. 2. The major components consisted of a heat source (combustor), a full annular vane row, an exhaust duct line, a quench system (to lower the temperature of the exhaust gas), and a vacuum exhaust system.

The vane row consisted of 36 stator vanes, separated into two groups: 10 test vanes and 26 slave vanes. The test vane and slave vane cooling air was supplied from two separate manifolds, with the flow rates to each manifold independently controlled. In these particular tests, the test vanes and the slave vanes had the same internal and external configuration.

The stator vane configuration, which was used for the results presented herein, is shown in Fig. 3. The internal heat transfer was simple convection without any augmentation normally found in modern turbine airfoils (i.e., impingement insert or turbulators) to simplify the instrumentation installation procedure. Cooling air was supplied to the vane through the vane tip and was exhausted into a plenum at the vane trailing-edge hub.

INSTRUMENTATION

The instruments used in the HSF cascade were exposed to an extremely hostile environment of high temperature, pressure, and heat flux. As such, there were some unique conditions to be met. The material used had to be compatible with the base material of the turbine airfoil. The instruments had to survive in the extremely hostile environment. They had to be rugged to withstand the vibration generated in a turbine engine. The physical size of the instruments had to be small to obtain a reasonably acceptable spatial resolution and to minimize the impact on the parameter being measured. The instrumentation evaluated in this experiment consisted of both conventional instruments used in high-temperature tests and some advanced nonconventional instrumentation techniques. Conventional instrumentation is defined here as temperature and pressure measurements using sheathed thermocouples and strain gage pressure transducers.

Nonconventional Instrumentation

Nonconventional instrumentation is defined here as any instrumentation advanced in either function or design beyond the conventional high temperature and pressure sensors. Among these would be heat flux gages (Gardon type and paired thermocouples type), thin-film thermocouples, and the dual-element, fast-response gas temperature probe. The following subsections give a description of the instruments used in these experiments.

The heat flux gages used in these tests were developed under NASA contract, and reported by Atkinson, Cyr, and Strange (1984) for gas turbine applications. Two types of heat flux gages were installed on the airfoils: the Gardon gage and the paired thermocouple gage.

Gardon gage. The Gardon gage consists of a thin circular foil placed normal to the incidence heat flux and a peripheral heat sink. Heat flux entering the foil flows radially outward from the center of the foil towards the peripheral heat sink. The heat flux is proportional to the temperature difference between the center of the foil and the heat sink. Gardon gages have a long history, but the present application is quite unique. Figure 4 shows a schematic of the
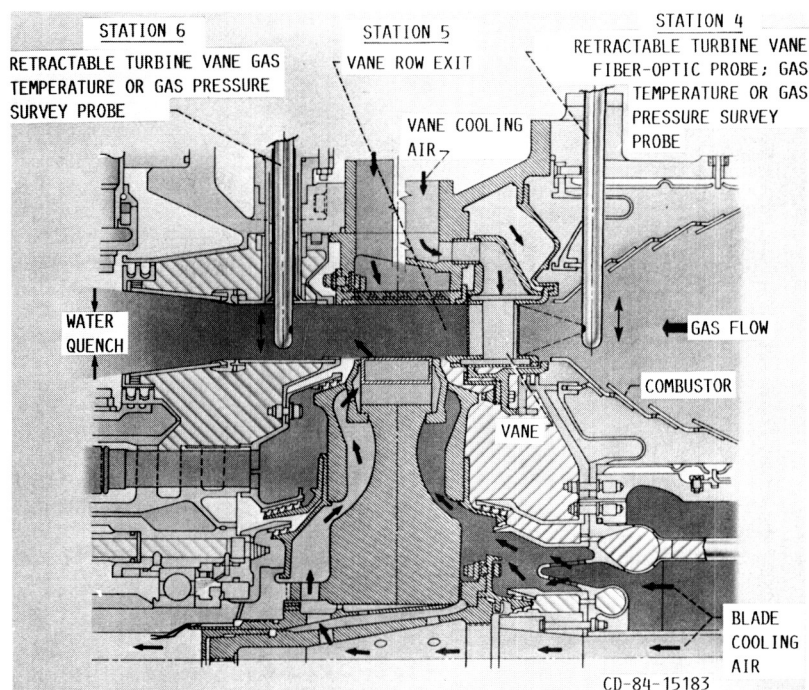

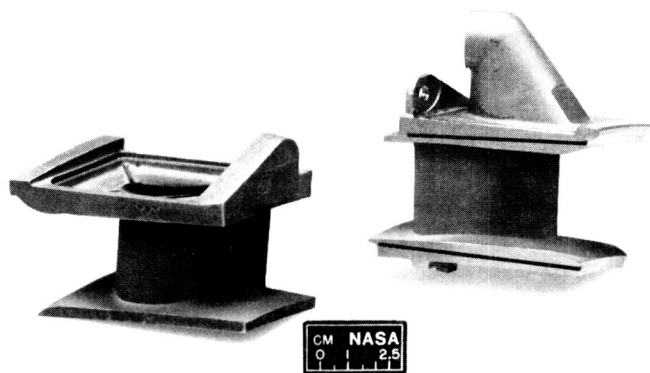Fig. 2 Cascade schematic cross section of combustor and cascade vane row

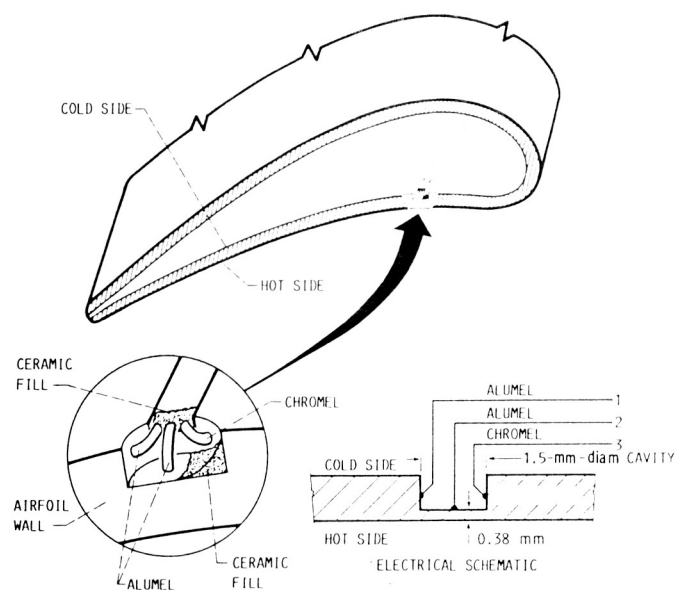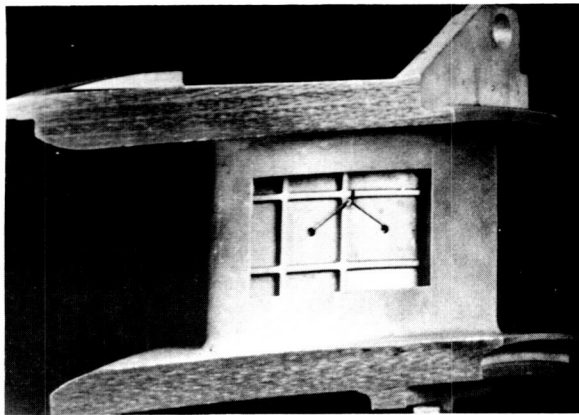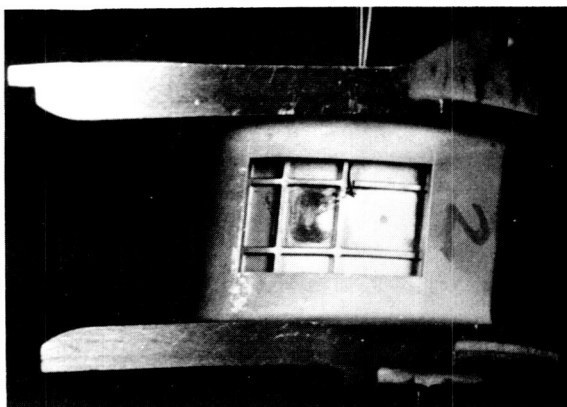Fig. 3 Vane airfoil used in Hot Section Facility cascade tests

Fig. 4 Schematic of Gardon gage heat flux sensor used in Hot Section Facility (wires 1 and 2 measure sensor output; wires 1 and 3 measure reference temperature)
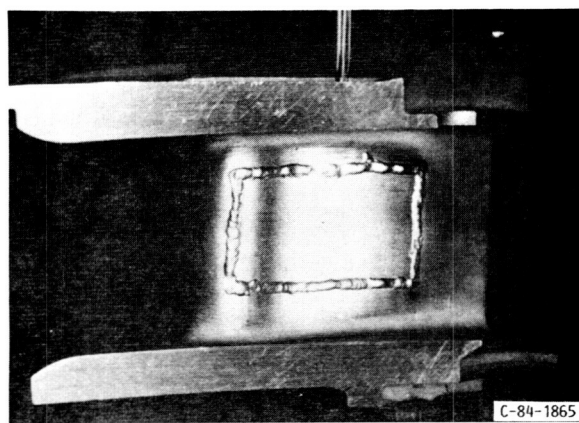
3

(a) VANE WITH WINDOW REMOVED (MACHINING OF CAVITIES FOR SENSORS AND GROOVES FOR SENSOR LEADS COMPLETE)

(b) VANE WITH LEADS INSTALLED (CERAMIC NOT YET INSTALLED AND SURFACE NOT YET SMOOTHED)

(c) VANE WITH WINDOW REWELDED INTO PLACE (VANE SURFACE WILL BE SMOOTHED BEFORE INSTALLING IN CASCADE)

Fig. 5 Installation of Gardon gage heat flux sensor

Gardon gage used in the HSF. This construction makes use of the airfoil material as an integral part of the gage itself to insure that the presence of the gage does not affect the local heat transfer rate because of its thermal properties or aerodynamic discontinuities. The differential temperature between the "foil" and the main airfoil body was obtained from two Alumel wires, one located at the center of the "foil" inside the cavity, and one at the side of the cavity wall (wires 1 and 2 in Fig. 4). The gage temperature level

was obtained with a pair of Chromel-Alumel wires located on the sides of the cavity wall (wires 1 and 3 in Fig. 4).

Installing the heat flux gage involved the removal of a window from the airfoil suction surface (Fig. 5(a)). The gage was then installed through the window on the now exposed internal pressure surface. A cavity, located on the cold side of the gage, was machined into the airfoil, leaving a thin layer (0.38 mm) of the airfoil material to serve as the foil. After installation of the thermocouple wires, the cavity was filled with ceramic cement to provide a smooth internal flow path as well as support and oxidation protection for the fine thermocouple wires (fig. 5(b)). After installation of the heat flux gage, the window was welded to the airfoil to again form the whole vane (Fig. 5 (c)). The welding was then smoothed to form a continuous airfoil surface. The gage, now an integral part of the vane, was calibrated in accordance with procedures outlined by Atkinson et al. before being installed in the cascade. A known normal incident heat flux was applied to each gage location, and the resulting output of the device was recorded. Figure 6 shows typical results of the calibration. The gage calibration uncertainty was within ±5 percent of the full-scale reading. Instrumentation uncertainty estimates are summarized in Table I.
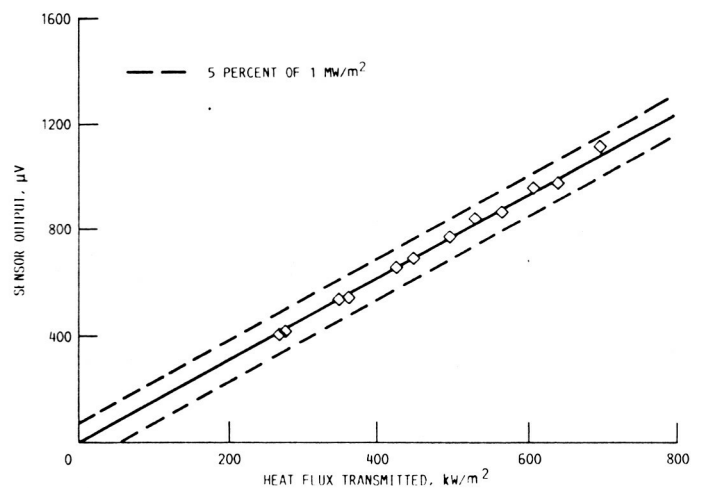

Fig. 6 Typical calibration data for Gardon gage heat flux sensors installed in vanes for Hot Section Facility

TABLE I. - MEASUREMENT UNCERTAINTY

Measurement	Uncertainty, percent	
	Instrument	Overall
Gas temperature		
Aspirated probe	±<1.0	±<1.0
Dual-element probe	±3.3	±3.3
Wall temperature		
Embedded thermocouple	±<1.0	±<1.0
Thin-film thermocouple	±1.6	±1.6
Heat transfer coefficient		
Gardon gage	±5	±11
Paired thermocouples	±5	±11
Thin-film thermocouple dual-element probe	-----	±15.3
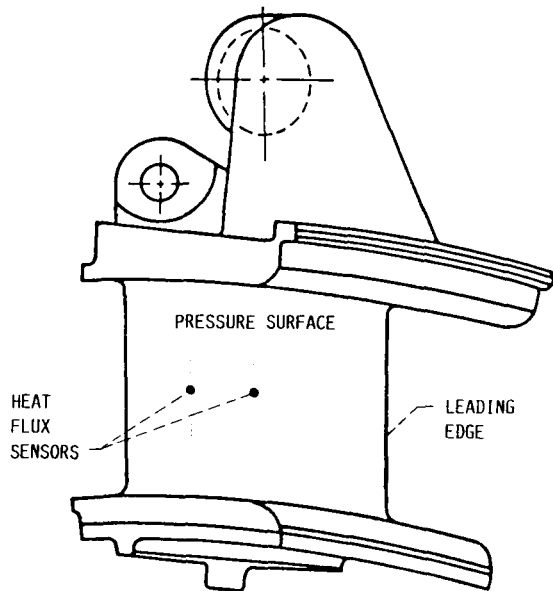
(a) GARDON GAGE AND PAIRED THERMOCOUPLE HEAT FLUX SENSOR LOCATIONS ON VANE
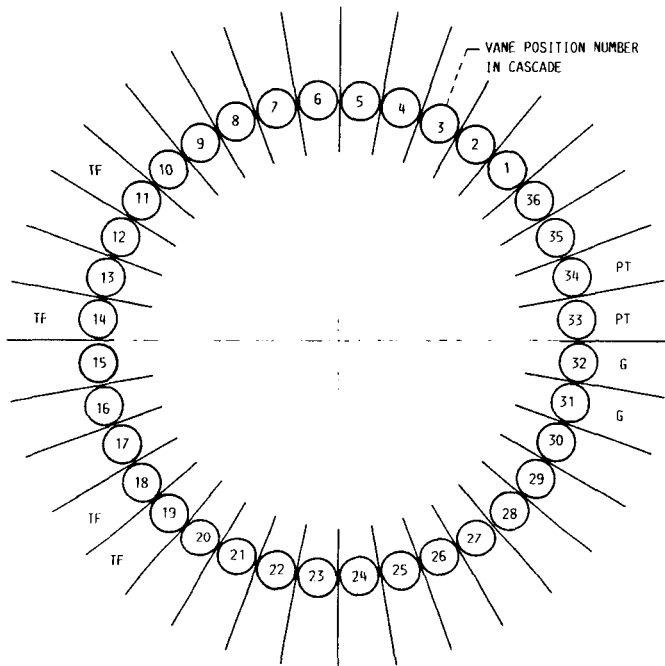
(b) NONCONVENTIONAL INSTRUMENTATION LOCATION IN CASCADE

Fig. 7 Heat flux sensor locations on vane and relative location of other nonconventional instrumentation in cascade (view looking downstream; Gardon gages, paired thermocouples, and thin-film thermocouples are labeled G, PT, and TF, respectively)

Four Gardon gages were installed on the pressure surface of two airfoils. These instrumented airfoils were located circumferentially at about 260° counterclockwise (ccw) from top dead center, at vane positions 31 and 32. Figure 7(a) shows the location of the gages on the vane. Figure 7(b) shows the relative location of the Gardon gage in the vane cascade.

Paired thermocouples. The paired thermocouple heat flux gage used three single, sheathed thermal elements embedded in the grooved surface of the vane airfoil (Fig. 8). Two of the conductors (Chromel and Alumel) were located on the cold side of the airfoil, while the third (Alumel) was located on the hot surface. The Chromel-Alumel thermal elements provided the local reference temperature, and the gage output was obtained as a differential signal from the pair of Alumel wires. The installation of these paired thermocouple heat flux gages was similar to that of the Gardon gages shown in Fig. 5. A window on the vane suction surface was removed, and the gage was installed in the exposed pressure surface. The window piece that was removed was then rewelded to the airfoil to again form the complete airfoil. These gages were also calibrated in accordance with procedures outlined by Atkinson et al. (Fig. 9). The gage calibration uncertainty was within ±5 percent of the full-scale reading.

The paired thermocouple airfoils were located at about 280° ccw from top dead center, at vane positions 33 and 34. The relative location of these airfoils within the vane row is also shown in Fig. 7(b).

Thin-film thermocouples. Thin-film thermocouples were surface-mounted thermocouples formed by depositing (by sputtering) a thin layer of electrical insulating material on the vane surface, and then depositing a metallic thermocouple material only a few microns thick on top of the insulating material. A typical application of the thin-film thermocouples is shown in Fig. 10. The installation procedure is discussed in detail by Grant et al. (1982). The thermal elements were platinum/platinum 10 percent rhodium (type S). Each thermal element of the thermocouple was ≈1.27 mm wide by 12 μm thick, forming a junction of ≈1.27 mm in the chordwise direction. A 2.5- to 3.0-μm-thick substrate of Al_2O_3 served as an insulator between the thin film and the airfoil wall. The junction between the thin film and the lead wire was formed by a hot compression technique described by Grant and Przybyszewski (1980). They found that a durable junction was formed by compressing the lead
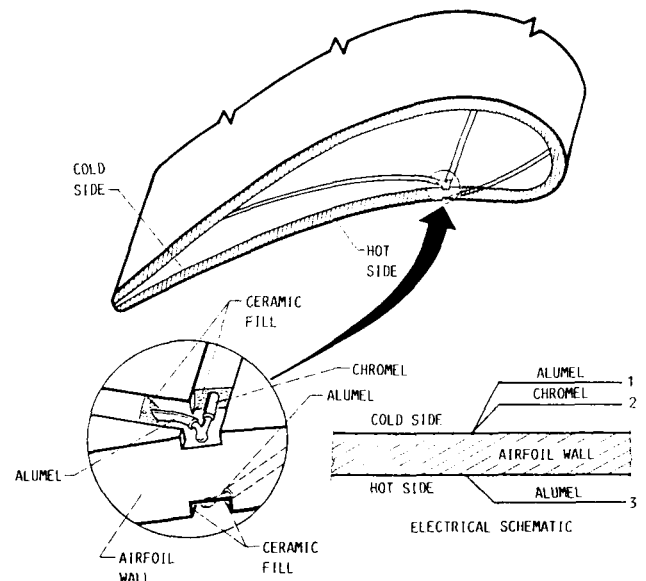

Fig. 8 Schematic of paired thermocouple heat flux sensor used in Hot Section Facility (wires 1 and 3 measure sensor output; wires 1 and 2 measure reference temperature)
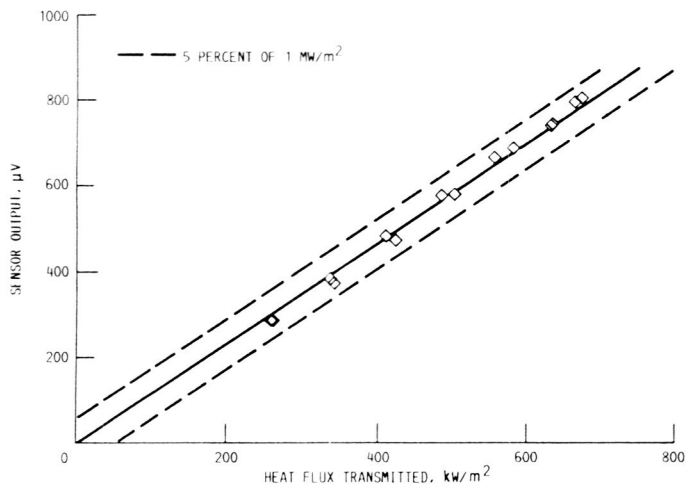
5

Fig. 9 Calibration data for paired thermocouple heat flux sensors installed in vanes for Hot Section Facility

Fig. 11 Thin-film thermocouple distribution on vanes
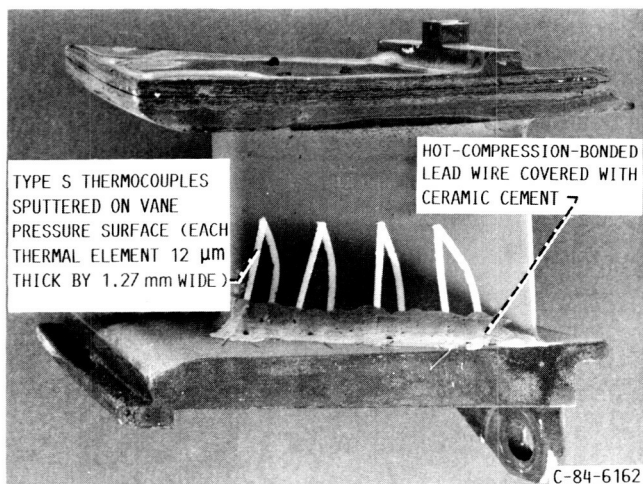

Fig. 10 Typical thin-film thermocouple installation on airfoil pressure surface (lead wires not attached)

wire onto the thin film until it plasticly deformed, and then heating the system to create a diffusion-bonded connection. Typically, this installation procedure results in a measurement uncertainty of 1.6 percent of the reading (in Celsius).

Twenty-four thin-film thermocouples were installed on the surfaces of four vanes. These vanes were located circumferentially at ≈60°, 90°, and 135° ccw looking downstream (0° at top dead center). Typically there were four thermocouples on one surface of the airfoil, and two thermocouples on the opposite surface. The distribution of the thin-film thermocouples is shown in Fig. 11.

Dual-element, fast-response gas temperature probe. The dual-element, fast-response gas temperature probe, located at the combustor exit, was the primary gas temperature instrument used to measure the fluctuations in the gas temperature. The probe, developed under NASA contract and reported by Elmore et al. (1983), is shown in Fig. 12. The two thermal elements of the probe were platinum 30 percent rhodium and platinum 6 percent rhodium (type B) and

were 0.076 mm and 0.25 mm in diameter, respectively. The probe was designed to measure temperature fluctuations up to 1.0 kHz and, through a compensation technique described by Elmore et al., reflect the true peak-to-peak amplitudes of the fluctuations. Measurement uncertainties was estimated by Gladden and Proctor (1985) to be 3.3 percent.
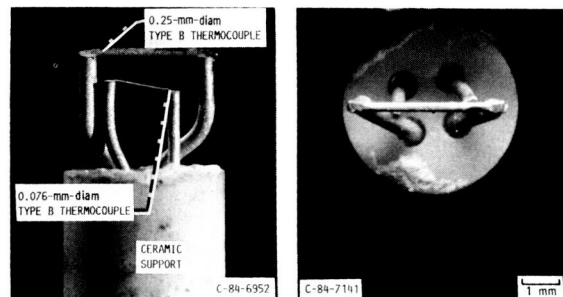

Fig. 12 Dual-element gas temperature probe

Conventional Instrumentation

The conventional instruments specific to the performance of the cascade measured the vane airfoil metal temperatures and the gas path temperatures and pressures. A cross-sectional schematic of the vane airfoil is given in Fig. 13, showing a composite summary of instrument locations on the airfoil. The locations shown in the figure represent either metal temperature or static pressure measurements. Because each airfoil could accommodate only a limited number of instrument grooves, the temperature or pressure distributions reported were composed of measurements from several airfoils in the annulus. It is worthy of note that even conventional instrumentation is a challenge, as shown in the next section.

Embedded thermocouples. Sheathed thermocouples embedded in the airfoil wall, a widely used method, were also used herein to measure metal airfoil temperatures. This method involved cutting grooves into the airfoil surface and then embedding the sheathed thermocouples into the grooves. The grooves were then covered with a metallic foil flush with the airfoil surface and spot welded in place. Figure 14 shows a typical installation of this type of surface temperature measurement. The thermocouple was formed by a pair of sheathed, single wires, and flattened at the junction. By using premium grade type K thermocouple wire, the overall measurement uncertainty was estimated to be less than 1.0 percent of the reading. However, this technique, described by Crowl and Gladden (1971), has its disadvantages. The presence of the grooves in the airfoil distorts the isotherms, while the thermocouple junction, formed below the airfoil surface, does not measure the airfoil surface temperature. Also, the decreased thickness of the airfoil wall weakens the structural integrity of the airfoil.
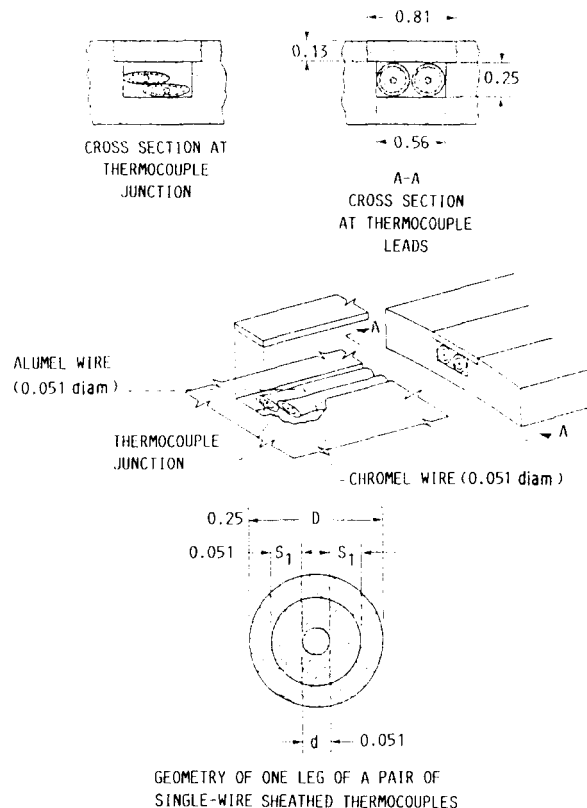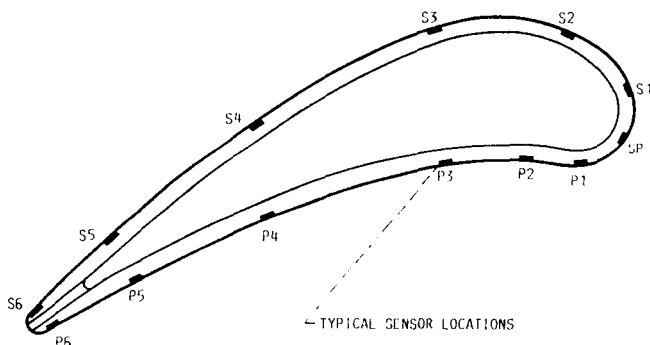

Fig. 14 Typical embedded thermocouple installation in metal wall of airfoil (all dimensions in millimeters)

Fig. 13 Vane airfoil cross section showing a composite of embedded thermocouple or pressure tap locations

SUCTION SURFACE		PRESSURE SURFACE	
SENSOR	X/L	SENSOR	X/L
SP	0.0		
S1	.067	P1	0.083
S2	.188	P2	.174
S3	.346	P3	.314
S4	.612	P4	.587
S5	.836	P5	.826
S6	.972	P6	.973

Aspirated gas temperature probe. The aspirated temperature probe was used for measuring high gas temperatures at steady-state conditions. This measurement technique was based on a design initially developed by Glawe et al. (1956). The sensing thermocouple element, located inside a metal tube, was shielded to minimize radiation heat loss and provided a stagnation condition. The mainstream gas was aspirated into the cylinder housing through a hole located on the side of the cylinder and stagnated in the cavity with the sensing thermocouple. Figure 15, taken from the report by Glawe et al., shows a typical double-shielded aspirated probe in which the sensing thermocouple was shielded in a second cylinder located within the first cylinder. The thermal element used in this probe was type R, which provided temperature measurement capability up to 1900 K. In addition, an iridium 40 percent rhodium versus iridium thermal element was available to extend the measurement capability up to 2200 K. The measurement uncertainty of this type of probe, after corrections for systematic errors, was estimated to be less than 1.0 percent.

DATA ACQUISITION

The operation and data acquisition for the facility were fully automated through an integrated digital computer system called the Digital Control Center (DCC). The four minicomputers in the DCC were interconnected; however, each computer had a dedicated task. The computers were labeled, according to their primary task, "Input," "Control," "Operations," and "Research." The main task of the research computer was to gather large volumes of research data and con-
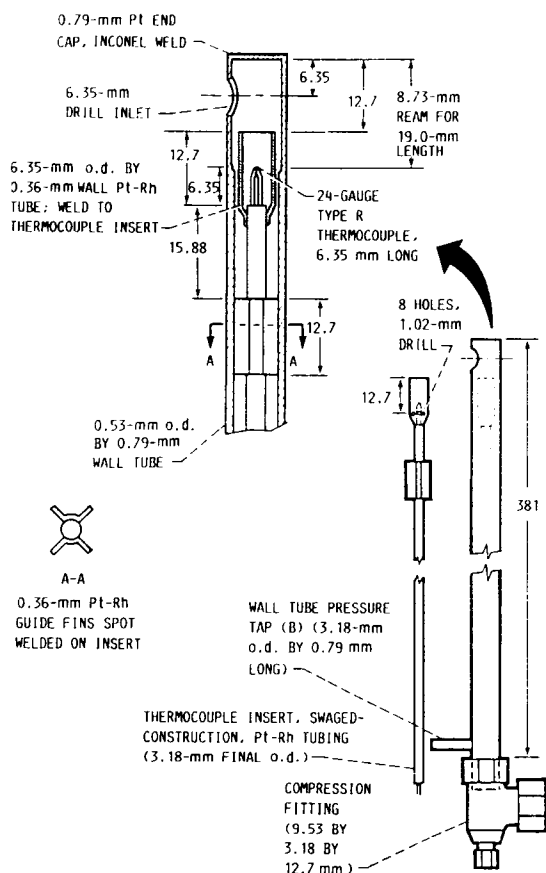
Fig. 15 Typical double-shielded aspirated probe (all dimensions in millimeters)

The diagram labels (left to right, top to bottom):
- 0.79-mm Pt END CAP, INCONEL WELD
- 6.35-mm DRILL INLET
- 6.35-mm o.d. BY 0.36-mm WALL Pt-Rh TUBE; WELD TO THERMOCOUPLE INSERT
- 6.35
- 12.7
- 8.73-mm REAM FOR 19.0-mm LENGTH
- 12.7
- 6.35
- 15.88
- 24-GAUGE TYPE R THERMOCOUPLE, 6.35 mm LONG
- 8 HOLES, 1.02-mm DRILL
- 12.7
- 12.7
- A
- A
- 0.53-mm o.d. BY 0.79-mm WALL TUBE
- 381
- A-A
- 0.36-mm Pt-Rh GUIDE FINS SPOT WELDED ON INSERT
- WALL TUBE PRESSURE TAP (B) (3.18-mm o.d. BY 0.79 mm LONG)
- THERMOCOUPLE INSERT, SWAGED-CONSTRUCTION, Pt-Rh TUBING (3.18-mm FINAL o.d.)
- COMPRESSION FITTING (9.53 BY 3.18 BY 12.7 mm)

vert them into engineering units. These research data were also fed into a large mainframe computer where more complex calculations and graphics operations were performed. More detailed description of the Digital Control Center is given by Gladden et al. (1985). In addition, transient data were acquired on an FM tape recorder. The analog output from the thin-film thermocouples and the dual-element temperature were recorded for postprocessing to determine compensated, peak-to-peak, time-resolved gas temperatures as well as surface heat flux. These results were reported by Gladden and Proctor.

DATA REDUCTION AND ANALYTICAL COMPARISON PROCEDURES

Gas-Side Heat Transfer Coefficient

Experimental heat transfer coefficients were obtained from the Gardon gages and the paired thermocouple gages by the following method

$$ h = \frac{Q/A}{\bar{T}_g - T_w} \qquad (1) $$

where the heat flux Q/A is determined from the gage calibration, T_w is the gage reference temperature, and $\bar{T}_g$ is the computed mean radius total gas temperature.

Gladden and Proctor also used the thin-film thermocouples and the dual-element gas temperature probe to determine experimentally the gas-side heat transfer coefficients. By assuming a semi-infinite solid, the

heat transfer coefficient can be related to the amplitude of the Fourier components of the surface temperature and the gas temperature by the approximation

$$ \frac{T_w(f)}{T_g(f)} = \frac{h_g}{\sqrt{2\pi f \rho C_p k}} \qquad (2) $$

The ratio $T_w(f)/T_g(f)$ was determined by computing the transfer function between the time-resolved wall temperature and the gas temperature.

A widely used boundary layer code, STAN5 (Crawford and Kays, 1976), was used to calculate the expected heat transfer coefficient distribution around the airfoil in order to provide a baseline for comparison of results. In this calculation, the flow near the leading edge was forced to be turbulent.

Gas Temperature Profile

The combustor exit radial gas total temperature profile was obtained by averaging temperatures from two traversing aspirated probes. The probes were located one vane chord in front of the cascade vane row at station 4 (vane inlet), at 263° ccw and 345° ccw respectively, from top dead center. The third traversing probe was used to measure total gas pressure. Data were taken in five radial steps from vane hub to tip. An average radial total temperature profile and an overall average total gas temperature were determined from these measurements. The measured temperature was corrected for radiation, conduction, and recovery losses by the method of Glawe et al. In addition, a theoretical combustor exit temperature was also determined in accordance with the method described by Svehla and McBride (1973). A calculated mean-radius total gas temperature was determined by multiplying the average measured mean-radius temperature by the ratio of the measured average temperature and the calculated average temperature.

Reynolds Number

The exit gas Reynolds number is calculated from the vane row inlet total temperature and pressure, the vane row exit static pressure, and the vane true chord length. The gas properties are based on the exit gas static temperature, derived from the exit static to inlet total pressure ratio.

$$ Re = \frac{(\rho V)_e C}{\mu} \qquad (3) $$

where, by assuming $P_4' = P_5'$,

$$ (\rho V)_e = P_4' \left(\frac{P_5}{P_4'}\right)^{1/\gamma} \left[\frac{2\gamma}{\gamma - 1} \frac{g_c}{R\bar{T}_{g,cal}} \left(1 - \left(\frac{P_5}{P_4'}\right)^{(\gamma-1)/\gamma}\right)\right]^{1/2} \qquad (4) $$

RESULTS AND DISCUSSION

Surface Temperatures

Thin-film thermocouples. Figure 11 shows the location of the thin-film thermocouples distributed on four airfoils. The circumferential positions of these airfoils within the vane cascade are shown in Fig. 7(b). Figure 16 shows a plot of the surface temperatures measured by all functioning thin-film thermocouples (open symbols) as a function of the
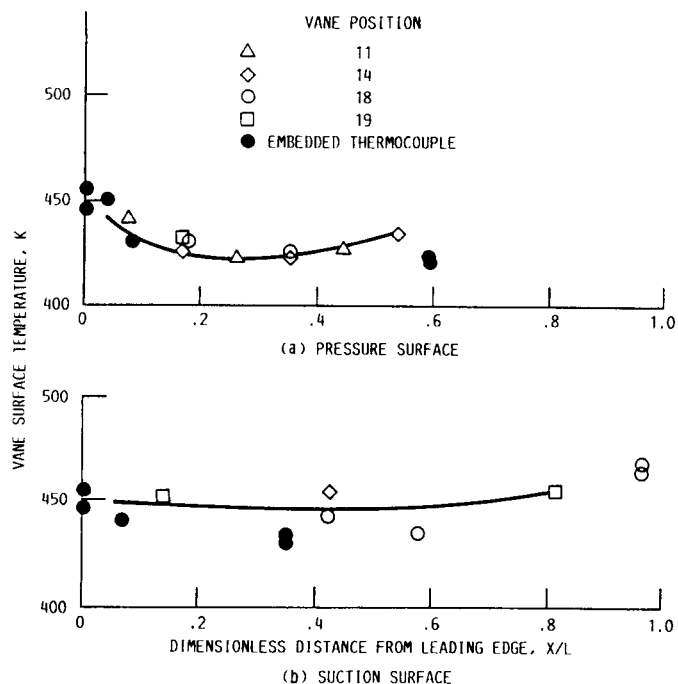
Fig. 16 Vane surface temperature from thin-film and embedded thermocouples (Re = 1.2×10^6)

dimensionless distance X/L. Also shown are temperatures from the embedded thermocouples (solid symbols). The data were taken at isothermal conditions, and at a Reynolds number of 1.2×10^6; that is, the gas stream was at a nearly uniform temperature. This condition was chosen in order to eliminate the effect of pattern factor in the combustor exit temperature. As generally expected, the figure shows that a cooler region existed in the midchord area, and hotter regions existed in the leading- and trailing-edge regions.

There was some data scatter among the thin-film thermocouple measurements; however, it was generally within the uncertainty of the measurements themselves. The embedded thermocouples generally indicated a somewhat lower temperature than the thin-film thermocouples. Some of the data scatter may also be attributed to the uncertainty in the uniformity of the coolant flow distribution among the vanes. This uncertainty could result in a greater or lesser degree of internal cooling, which could also contribute to the variation from point to point. However, this reflects, in part, the challenge of making and interpreting measurements in a realistic engine environment.

Of the 24 thin-film thermocouples installed, 1 was defective from the beginning, and another developed a secondary junction at the diffusion bonding surface in the early stages of the tests. Six other thin-film couples were later disabled at various stages of the test program, but valuable data were obtained before they were disabled. Of the disabled thin-film couples, two on the suction surface failed at the diffusion bond. Three of the thin-film couples, all on the pressure surface, failed because of a broken thin-film element. The fourth failed thin-film couple, on the suction surface, was due to a broken lead wire. All of the remaining thin-film couples functioned successfully until the end of the test program (35 hr of test time). A summary of the history of these thin-film couples is shown in Table II.

Embedded Thermocouples. Only a few embedded thermocouples were installed on these airfoils for this series of tests. As mentioned in the preceding subsection, the data from the embedded thermocouples are superimposed on the thin-film thermocouple plots in Fig. 16. The thermocouple measurements on the pressure surface and the suction surface agreed well with the thin-film couple measurements. The embedded thermocouples, however, indicated a slightly cooler temperature than that indicated by the thin-film couples. Intuitively, the temperatures of the embedded thermocouples should be lower than those indicated by the thin-film thermocouples because of the temperature gradient through the wall. Consequently, it is felt that both types of thermocouples are capable of providing metal temperature measurements within their limits of uncertainty.

Heat Flux Measurements
Figure 17 shows the experimental heat transfer coefficient distribution on these airfoils for a Reynolds number of 1.2×10^6 compared with that predicted by the STAN5 boundary layer code. Included are data from thin-film thermocouples (gages), Gardon gages, and paired thermocouples. The results of this comparison are discussed in the following paragraphs.

Gardon Gage. Two Gardon heat flux gages were installed on the pressure surface of each of two airfoils. One of the gages was inoperative from the beginning of the test program. A second gage developed a secondary junction early in the test program, and gave unreliable results. The remaining two gages, both located on the same vane, functioned successfully until the end of the test program. These gages were installed on the pressure surface of vane 31. (The relative location of vane 31 in the cascade is shown in Fig. 7(b)). The experimental heat transfer coefficients for a Reynolds number of 1.2×10^6, obtained from the Gardon gage, are shown in Fig. 17(a). The data are plotted as a function of the dimensionless distance X/L. These data were not corrected for

TABLE II. – THIN-FILM THERMOCOUPLE FAILURE ANALYSIS

Vane position	Sensor	Failure mode	Time, hr
11	TTF07	At diffusion bond	9 1/6
	08	At diffusion bond	1 3/4
	09	(a)	(a)
	10	(a)	(a)
	11	(a)	(a)
	12	"Pig tail" missing	0
14	TTF19	(a)	(a)
	20		
	21		
	22		
	23		
	24	One leg of thermocouple missing	21 3/4
18	TTF31	(a)	(a)
	32		
	33		
	34		
	35		
	36	One leg of thermocouple missing	19
19	TTF25	(a)	(a)
	26	Broken Pt lead wire	17
	27	Secondary at diffusion bond	0
	28	(a)	(a)
	29	(a)	(a)
	30	Break in thermocouple leg	29 3/4

aFunctioning until end of test (35 hr).

9

(a) PRESSURE SURFACE

(b) SUCTION SURFACE
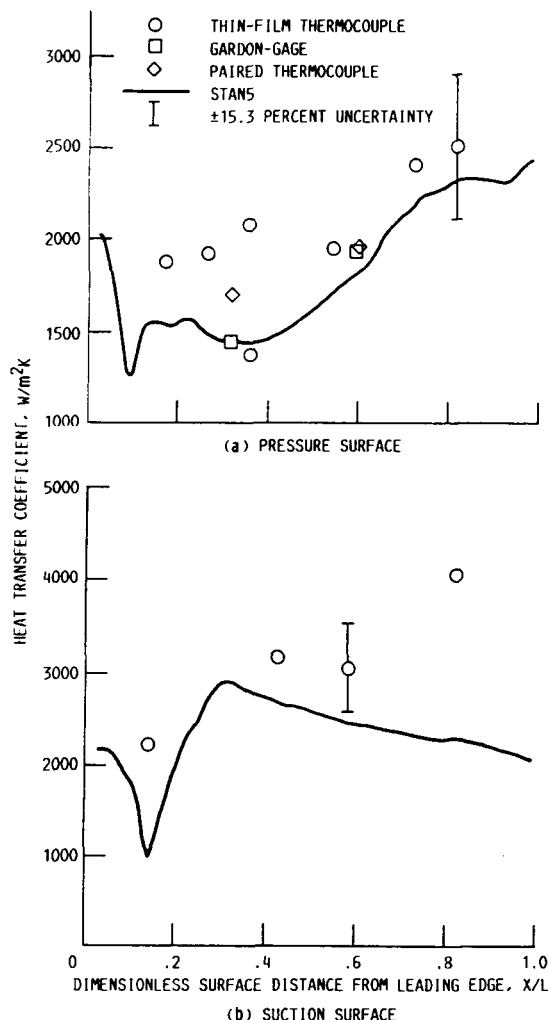
Fig. 17 Experimental heat transfer coefficients compared with STAN5 predictions (Re = 1.2x10^{6})

(a) THIN-FILM THERMOCOUPLE (TTF10) RESPONSE TO GAS TEMPERATURE RAMP

(b) GAS TEMPERATURE RAMP MEASURED BY 0.025 cm ELEMENT OF DUAL-ELEMENT PROBE

Fig. 18 Typical time histories of gas and wall temperatures during 2 and 4 sec ramp cycles (Re = 1.2x10^{6})

radiation or conduction errors, since the radiation component was less than 2 percent, and the conduction error was estimated to be much less than 1.0 percent (Gladden et al., 1971). The predicted heat transfer coefficient distribution from the STAN5 boundary layer code is also shown. The heat transfer coefficients from the Gardon gages agreed fairly well with the predicted values from STAN5. The measurement uncertainty was estimated to be approximately ±11 percent for the Gardon gages. The primary component of this uncertainty is the uncertainty of the gas temperature at the gage location, which was estimated to be as great as ±5 percent.

Paired thermocouples. Two paired thermocouple heat flux gages were also installed on the pressure surface of each of two airfoils. These functioned successfully throughout the experiment. Figure 17 also shows the experimental heat transfer coefficients from these gages, and the comparison with the STAN5 predictions is fairly good. The measurement uncertainty for these gages was also estimated to be approximately ±11 percent. The heat transfer coefficients from the Gardon gage as well as from the paired thermocouples, as obtained from the steady-state tests, agreed well with the analytical solutions.
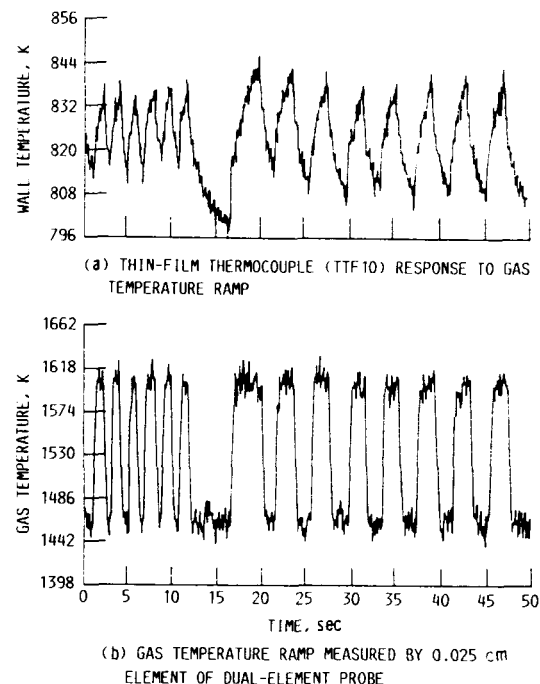
Thin-film thermocouples. Low-frequency variations (<1 Hz) of the gas stream temperature were imposed on the cascade. The responses of the thin-film thermocouples to the imposed variations of the gas temperature were used to determine the heat transfer coefficients, as was reported by Gladden and Proctor. These temperature oscillations, shown in Fig. 18, were used to determine the heat transfer coefficients. These results are also shown in Fig. 17. On the pressure surface (Fig. 17(a)), the experimental heat transfer coefficients generally agreed with those predicted from the STAN5 boundary layer code, at least in trend. The deviations of these data from the previous results and from analysis near the leading edge may be due to boundary layer transition or boundary layer separation. In any event, these sensors apparently measured a real phenomenon. On the suction surface (Fig. 17(b)), the heat transfer coefficients obtained from the thin-film thermocouples agreed with the STAN5 predictions, with the exception of one data point at the trailing edge (an X/L value of 0.82). Gladden and Proctor noted that it is not uncommon for there to be a sudden increase in heat transfer coefficient at the suction surface trailing edge, possibly due to secondary flow effects. Considering the experimental uncertainty of ±15 percent, based primarily on the uncertainty in the transfer function, the agreement is regarded as good.

This technique has been shown to be a good method of measuring the heat flux in a high temperature and pressure environment. Better resolution could be obtained by reducing the size of the thermocouple junction and increasing the density of sensors on a given airfoil.

Gas Temperature Measurements

Dual-element probe. Figure 19 shows a typical, time-resolved, compensated, gas temperature fluctuation as measured by the dual-element probe. These
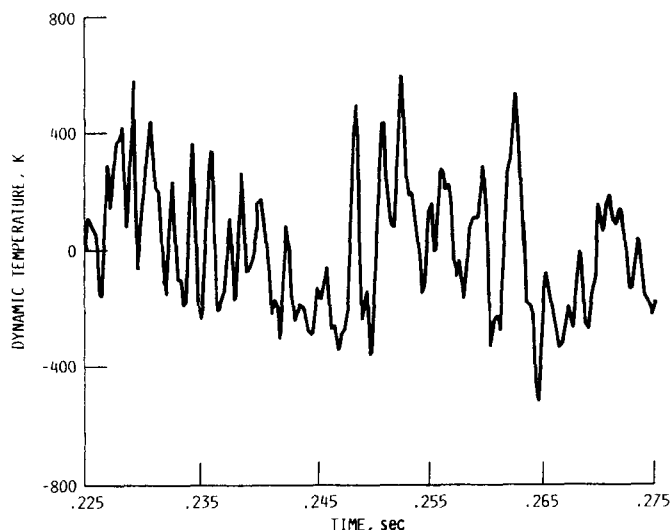
10

Fig. 19 Typical time-resolved, compensated, gas temperature fluctuation (76-μm thermocouple, partial time record for 1159 K)

data are taken from combustor experiments reported by Elmore et al. The overall peak-to-peak amplitude of the temperature measurement was 1250 K superimposed on a mean temperature of 1150 K. The maximum uncertainty of the fluctuation component is 3 K/$\sqrt{Hz}$. At the design frequency of 1 kHz, this uncertainty is about 30 K. This probe was used to obtain heat transfer coefficient measurements in conjunction with the thin-film thermocouples. However, the high-frequency data from these experiments has not yet been compensated to provide the true peak-to-peak temperature oscillation characteristics of this combustor. It should be noted that the probe proved to be durable, and survived the many thermal cycles in the hostile HSF environment.

Aspirated Probe. Figure 20, reproduced from Gladden et al. (1985) shows the mainstream gas temperature profile at the combustor exit. Measured temperatures from the aspirated probe are compared with unpublished results obtained from a research combustor of the same design and tested in the combustor research leg of the HSF. The research combustor test data were obtained from a complete circumferential and radial survey of the gas temperature at the combustor exit plane reported by Wear et al. (1983). Figure 20 shows the circumferentially averaged radial temperature profile and the maximum temperature profile obtained from this research combustor. The figure also shows the measured temperature profiles from two traversing aspirated temperature probes located at the combustor exit (stator inlet) plane of the cascade. A calculated temperature, based on combustor efficiency and a theoretical gas temperature, is also shown as a dashed line. The theoretical gas temperature is obtained from thermodynamic considerations of the fuel properties, the combustion air inlet temperature, and the fuel-to-air ratio from Svehla and McBride. The calculated temperature corresponds to that obtained from the research combustor for similar conditions.

The type R aspirated total temperature probes provide a good measurement of the gas stream temperature up to levels of 1980 K. However, because of the circumferential variations that exist in real high-temperature environments (i.e., pattern factor), it
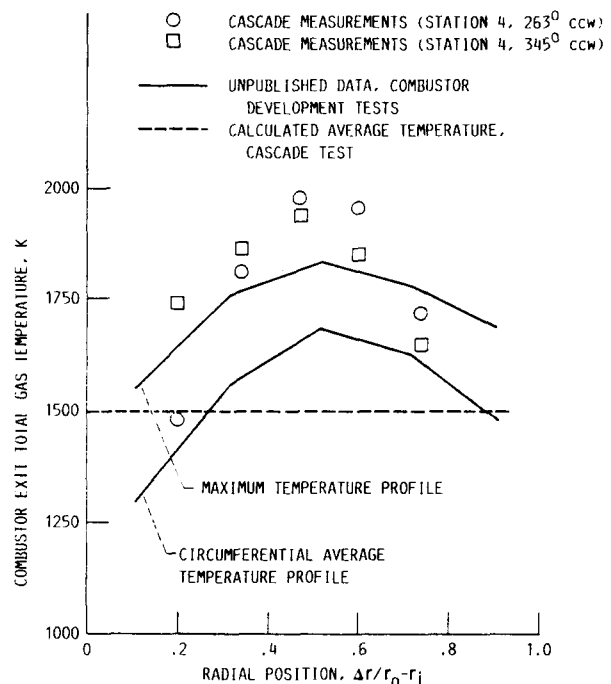

Fig. 20 Typical gas total temperature profile at station 4 (combustor exit; ccw is counterclockwise from top dead center, looking downstream)

is difficult to estimate the gas temperature at locations other than where probes are located.

Gas Pressure Measurement
The aerodynamic performance of the airfoil is characterized by the surface static pressure distribution shown in Fig. 21. Data are plotted for two different Reynolds numbers (0.55x10^{6} and 2.50x10^{6}) for the design flow conditions. Also shown is the design pressure distribution for this airfoil
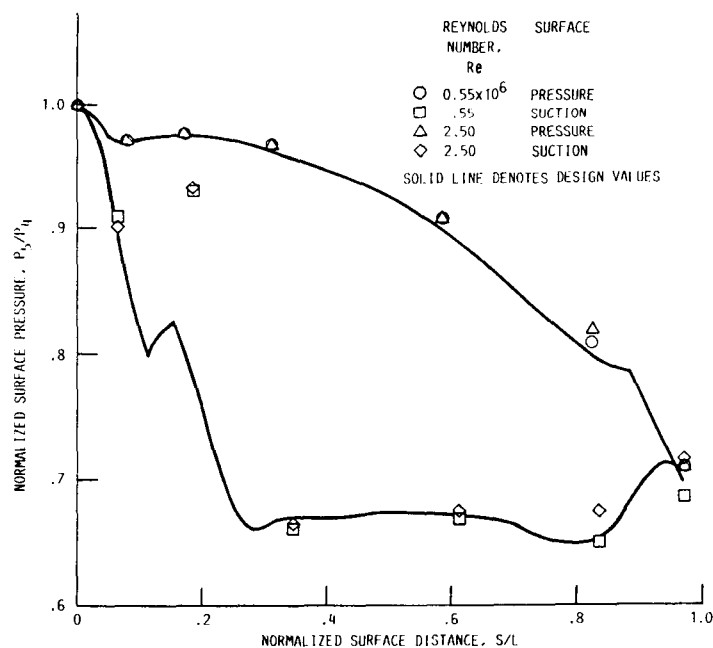

Fig. 21 Surface static-to-total pressure distribution (Re = 0.55x10^{6} and 2.50x10^{6})

11

reported by Whitney et al. (1967). With the exception of one point, at an X/L of 0.188 on the suction surface, the pressure distribution compares favorably with the predicted values. The agreement between experimental and predicted aerodynamic performance lends assurance that the operation of the cascade was satisfactory as the experimental data were being taken.

CONCLUDING REMARKS

Heat transfer research in a high-temperature, high-pressure gas turbine environment can be used as a code calibration experiment. Generally, code calibration can be accomplished if sufficient care and attention are given to the instrumentation installation techniques in a very challenging environment. These measurements must be made in a systematic, well-thought-out approach in order to obtain optimum results. The NASA Hot Section Facility has used both conventional and nonconventional instruments to demonstrate experimentally that these measurements can be made in an extremely hostile environment. Thin-film thermocouples were shown to be durable and to provide reliable vane surface temperature measurements throughout the test program. Heat flux gages, both the Gardon type and the paired thermocouples type, provided local, steady-state heat transfer coefficients. The dual-element, fast-response gas temperature probe, used in conjunction with the thin-film thermocouples, also provided a method of obtaining heat transfer coefficients. This technique provided data that generally agree with the steady-state measurements as well as with analytical predictions from the STAN5 boundary layer program. These nonconventional measurement techniques merit further study and development for use in a high-temperature, high-pressure gas turbine engine environment.

REFERENCES

Atkinson, W.H., Cyr, M.A., and Strange, R.R., 1984, "Turbine Blade and Vane Heat Flux Sensor Development," PWA-5914-21, Pratt and Whitney Aircraft, East Hartford, CT (NASA CR-168297).

Cochran, R.P., Norris, J.W., and Jones, R.E., 1976, "A High-Pressure, High-Temperature, Combustor and Turbine-Cooling Test Facility," ASME Paper 76-WA/GT-4.

Crawford, M.E., and Kays, W.M., 1976, "STAN5 - A Program for Numerical Computation of Two-Dimensional Internal and External Boundary Layer Flows," SU-HMT-23, Stanford University, Stanford, CA (NASA CR-2742).

Crowl, R.J., and Gladden, H.J., 1971, "Methods and Procedures for Evaluating, Forming, and Installing Small-Diameter Sheathed Thermocouple Wire and Sheathed Thermocouples," NASA TM X-2377.

Elmore, D.L., Robinson, W.W., and Watkins, W.B., 1983, "Dynamic Gas Temperature Measurement System, Vol. I - Technical Effort," PWA/GPD-FR-17145-Vol. 1, Pratt and Whitney Aircraft, West Palm Beach, FL (NASA CR-168267-VOL-1).

Gladden, H.J., Hippensteele, S.A., Hickel, R.O., and Dengler, R.P., 1971, "Radiation Heat Transfer Characteristics of Turbine Vane Airfoils in a Water-Cooled Cascade," NASA TM X-2203.

Gladden, H.J., and Proctor, M.P., 1985, "Transient Technique for Measuring Heat Transfer Coefficients on Stator Airfoils in a Jet Engine Environment," AIAA Paper 85-1471 (NASA TM-87005).

Gladden, H.J., Yeh, F.C., and Fronek, D.L., 1985, "Heat Transfer Results and Operational Characteristics of the NASA Lewis Research Center Hot Section Cascade Test Facility," ASME Paper 85-GT-82 (NASA TM-86890).

Glawe, G.E., Simmons, F.S., and Stickney, T.M., 1956, "Radiation and Recovery Corrections and Time Constants of Several Chromel-Alumel Thermocouple Probes in High Temperature, High Velocity Gas Streams," NACA TN-3766.

Grant, H.P., and Przybyszewski, J.S., 1980, "Thin Film Temperature Sensor - Phase I" PWA-5526-31, Pratt and Whitney Aircraft, Commercial Products Division, East Hartford, CT (NASA CR-159782).

Grant, H.P., Przybyszewski, J.S., Claing, R.G., and Anderson, W.L., 1982, "Thin Film Temperature Sensors, Phase III," PWA-5708-26, Pratt & Whitney Aircraft, Commercial Products Division, East Hartford, CT (NASA CR-165476).

Kline, S.J., and McClintock, F.A., 1953, "Describing Uncertainties in Single-Sample Experiments," Mechanical Engineering, Vol. 75, no. 1, p. 38.

Svehla, R.A., and McBride, B.J., 1973, "Fortran IV Computer Program for Calculation of Thermodynamic and Transport Properties of Complex Chemical Systems," NASA TN D-7056.

Wear, J.D., Trout, A.M., Smith, J.M., and Jacobs, R.E., 1983, "Preliminary Tests of an Advanced High-Temperature Combustion System," NASA TP-2203.

Whitney, W.J., Szanca, E.M., Moffitt, T.P., and Monroe, D.E., 1967, "Cold Air Investigation of a Turbine for High-Temperature-Engine Application. I. Turbine Design and Overall Performance," NASA TN D-3751.

1. Report No. NASA TM-102294	2. Government Accession No.	3. Recipient's Catalog No.
4. Title and Subtitle Experience With Advanced Instrumentation in a Hot Section Cascade		5. Report Date
		6. Performing Organization Code
7. Author(s) Frederick C. Yeh and Herbert J. Gladden		8. Performing Organization Report No. E-4962
		10. Work Unit No. 505-62-21
9. Performing Organization Name and Address National Aeronautics and Space Administration Lewis Research Center Cleveland, Ohio 44135-3191		11. Contract or Grant No.
		13. Type of Report and Period Covered Technical Memorandum
12. Sponsoring Agency Name and Address National Aeronautics and Space Administration Washington, D.C. 20546-0001		14. Sponsoring Agency Code

15. Supplementary Notes

Prepared for the 1989 Winter Annual Meeting of the American Society of Mechanical Engineers, San Francisco, California, December 10-15, 1989.

16. Abstract

The Lewis Research Center gas turbine Hot Section Test Facility was developed to provide a "real engine" environment with known boundary conditions for the aerothermal performance evaluation and verification of computer design codes. This verification process requires experimental measurements in a hostile environment. The research instrumentation used in this facility are presented, and their characteristics and how they perform in this environment are discussed. The research instrumentation consisted of conventional pressure and temperature sensors, as well as thin-film thermocouples and heat flux gages. The hot gas temperature was measured by an aspirated temperature probe and by a dual-element, fast-response temperature probe. The data acquisition mode was both steady state and time dependent. These experiments were conducted over a wide range of gas Reynolds numbers, exit gas Mach numbers, and heat flux levels. This facility was capable of testing at temperatures up to 1600 K, and at pressures up to 18 atm. These corresponded to an airfoil exit Reynolds number range of 0.5×10^6 to 2.5×10^6 based on the airfoil chord of 5.55 cm. Results are presented that characterize the performance capability and the durability of the instrumentation. Discussion will also be made on the challenge of making measurements in hostile environments. The instruments exhibited more than adequate durability to achieve the measurement profile. About 70 percent of the thin-film thermocouples and the dual-element temperature probe survived several hundred thermal cycles and more than 35 hr at gas temperatures up to 1600 K. Within the experimental uncertainty, the steady-state and transient heat flux measurements were comparable and consistent over the range of Reynolds numbers tested.

17. Key Words (Suggested by Author(s)) Heat transfer Turbine blades High temperature instrumentation	18. Distribution Statement Unclassified – Unlimited Subject Category 34

19. Security Classif. (of this report) Unclassified	20. Security Classif. (of this page) Unclassified	21. No of pages 14	22. Price* A03